Nanochem Res 2(2): 159-165, Summer and Autumn 2017

RESEARCH PAPER

The effect of cationic surfactant on the structure, morphology and optical band gap of ferrites synthesized by a microwave sol–gel auto-combustion method

Mahnaz Kamel Attar Kar [1], Faranak Manteghi [1]*, Reza Fazaeli [2], Mehdi Ghahari [3]

[1] *Department of Chemistry, Iran University of Science and Technology, Tehran, Iran*

[2] *Department of Chemical Engineering, Faculty of Engineering, South Tehran Branch, Islamic Azad University, Tehran, Iran*

[3] *Department of Nanomaterials and Nanocoatings, Institute for Color Science and Technology (ICST), Tehran, Iran*

ARTICLE INFO

Article History:
Received 15 April 2017
Accepted 2 June 2017
Published 1 July 2017

Keywords:
Band Gap
CTAB
Ferrites Nanoparticles
Microwave Sol-Gel Auto-Combustion Method
SDS

ABSTRACT

Cu and Ni ferrites as the semiconductor materials were synthesized by a microwave sol-gel auto-combustion method. Two cationic surfactants, sodium dodecyl sulfate (SDS) and cetyltrimethylammonium bromide (CTAB), were applied and the influence of surfactants on the properties of the Cu and Ni ferrite particles was studied. The samples were characterized by X-ray powder diffraction (XRD) pattern, scanning electron microscope analysis (SEM), Fourier transform infrared (FT-IR) spectroscopy and diffuse reflectance spectra (DRS). Powder XRD analysis and FT-IR spectroscopy confirmed the formation of ferrite spinel phase. The crystallite size was calculated to be 50-95 nm using Scherrer's equation. The morphology and size of the synthesized nanoparticles have been observed by scanning electron microscopy. The particles were agglomerated without using surfactant. Using CTAB leads to the samples with layer shapes, and using SDS leads to the samples with pyramidal shapes. The energy band gaps calculated from UV–DRS absorption by using Kubelka-Munk equation were 1.68-1.77 eV, indicating that band gap of Cu ferrites becomes small and band gap of Ni ferrites becomes large in the presence of surfactant.

How to cite this article
Kamel Attar Kar M, Manteghi F, Fazaeli R,Ghahari M. The effect of cationic surfactant on the structure, morphology and optical band gap of ferrites synthesized by a microwave sol–gel auto-combustion method. Nanochem Res, 2017; 2(2):159-165. DOI: 10.22036/ncr.2017.02.001

INTRODUCTION

Recently, magnetic nanoparticles (MNPs) have attracted huge interest from a broad range of usage, such as magnetic fluids, data storage, bio applications, drug delivery, and MRI, and unique magnetic properties such as superparamagnetism, high coercivity, low Curie temperature and high magnetic susceptibility. They are classified as good catalysts due to low-cost, green, efficient, and reusable catalysts and easy separation by using an external magnetic field. Ferrites are one of the important magnetic materials, because of their special properties like electrics, magnetic, optical and catalytic properties. These materials were used as catalyst because of excellent catalytic activity, easy synthesis, nontoxic, reusability, economic viability, ecofriendliness, green, recyclable, and reusable catalyst. $CuFe_2O_4$ and $NiFe_2O_4$ have been chosen for their unique properties. Nickel ferrite has inverse spinel structure. Copper ferrite has two crystallographic spinel structures, the high temperature cubic phase and the low temperature tetragonal phase. Tetragonal phase has inverse spinel structure. Spinel ferrite structure had a

* Corresponding Author Email: *f_manteghi@iust.ac.ir*

chemical formula of MFe_2O_4, in which oxygen ions are placed in a fcc arrangement, and the metal ions occupy the spaces between them. These spaces are tetrahedral or A sites and octahedral or B sites. In normal spinel structure M^{2+} are on A sites and Fe^{3+} are on B sites but in inverse spinel structure M^{2+} are on B sites and Fe^{3+} are equally divided between A and B sites. The divalent and trivalent ions normally occupy the B sites in a random fashion [1-9].

There are various chemical and physical techniques to synthesize ferrites. The synthesis method determines the dimension and shape and properties of the nanostructure. Nanosized spinel ferrites can be prepared by like co-precipitation, solvothermal, hydrothermal, deposition–precipitation, electrochemical, high-temperature method, solid-state reactions, wet-chemical synthesis, auto–combustion method, Sol-gel, ultrasonic assisted and sonochemical method [10-21].

In this work ferrites nano particles are synthesized by a microwave sol–gel auto combustion method. The combustion process is an easy, safe, rapid and economic method used to synthesize nano ferrites [22]. The application of microwaves in the calcination process of inorganic materials has attracted much attention recently because it offers a novel synthesis pathway with notable features such as high purity, rapid heating rates, short processing durations, low power requirements, economical, and product uniformity. Different from conventional heating process, microwave heating is an in situ mode of energy conversion. Heat will be generated internally within the material, instead of originating from external sources. So, the microwave energy is transformed into heat energy by strong inter-molecular friction causing to increase the temperature of materials rapidly [23].

The incorporation of nanoscaled inorganic particles and organic materials (such as polymers) has been widely investigated, considering the extra advantages that could be obtained with combined properties of the inorganic materials (mechanical strength, magnetic and thermal stability) and the organic polymers (flexibility, dielectric, ductility and processability) [24]. Applying surfactants which are composed of molecules containing hydrophilic head and hydrophobic tail, along with sol–gel method can improve the properties of the synthesized powders. In the presence of surfactant, surface tension of solution is reduced and this facilitates nucleation and formation of

Table 1. Average size of the produced spinel ferrites.

Copper ferrite samples	Size/nm	Nickel ferrite samples	Size/nm
$CuFe_2O_4$	77	$NiFe_2O_4$	95
$CuFe_2O_4$/CTAB	50	$NiFe_2O_4$/CTAB	82
$CuFe_2O_4$/SDS	55	$NiFe_2O_4$/SDS	74

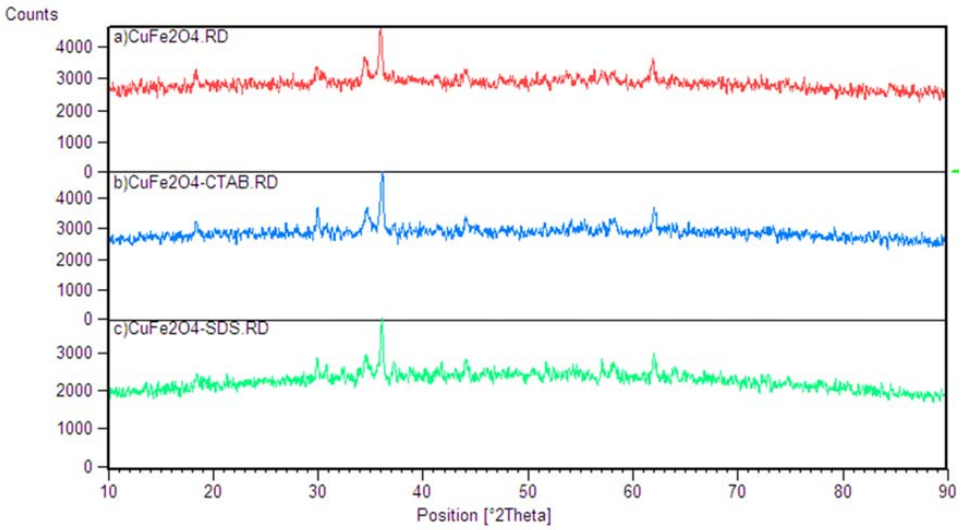

Fig. 1. XRD patterns of $CuFe_2O_4$ samples: a)$CuFe_2O_4$, b)$CuFe_2O_4$/CTAB & c)$CuFe_2O_4$/SDS.

the new phases. The formation of reverse micelles in gel can be effective in controlling the particles growth and the distance between particles [25].

In the present study, the microwave sol–gel auto-combustion method is applied for synthesizing the Ni and Cu ferrites using CTAB and SDS, and the effect of using surfactant on the properties of the prepared semiconductor samples is studied.

EXPERIMENTAL

Reagents

The chemical materials used in this work to prepare Ni and Cu ferrites using CTAB and SDS were $Fe(NO_3)_3{\cdot}9H_2O$, $Ni(NO_3)_2{\cdot}6H_2O$, $Cu(NO_3)_2{\cdot}6H_2O$, $C_6H_8O_7{\cdot}H_2O$, NH_4OH, sodium dodecyl sulfate (SDS) and cetyltrimethylammonium bromide (CTAB). All of the reagents used in the experiments are of analytical grade and used without further purification from Merck Chemical company (Germany).

Methods

Microwave synthesis was performed on a Solardom- LG (900 W). A STOE x-ray diffractometer revealed X-ray powder diffraction (XRD) pattern to determine the crystallinity and phase of the ferrite nanoparticles. A Philips SEM (LEO 1455VP) was used to obtain a scanning electron microscope analysis (SEM). Fourier transform infrared (FT-IR) spectroscopy was recorded on a Perkin-Elmer to analyze cubic spinel phase of nanoparticles and observe product after oxidation. Diffuse reflectance spectra (DRS) of the ferrite nanoparticles were measured on a Perkin-Elmer UV-VIS Instrument.

Synthesis of the samples

Appropriate amounts of metal nitrates and citric acid were first dissolved in a minimum amount of deionized water. The molar ratio of nitrates to citric acid was 1:1. A small amount of ammonia was added to the solution to adjust the pH value at about 7. The stoichiometric amount of surfactant was dissolved in minimum amount of water, added to the above solution. Then, the mixed solution was poured into a dish and heated at 80°C and stirred to transform into a xerogel. Dry gels were subjected to microwave irradiation (10 at 900 W) until the solution boiled. When ignited points were observed, the dried gel burnt in a self-propagating combustion manner until all the gel was burnt out completely to form a loose powder. During combustion large amounts of gas were given off and a lightweight massive powder formed quickly. The powder was then calcined at 800°C for 2 h to remove any organic material [23, 26 & 27].

RESULTS AND DISCUSSION

XRD analysis

X-ray diffraction patterns of the various calcined precursors are shown in Figs. 1 and 2. The patterns indicate the formation of single-phase spinel ferrites by the conventional route (Fig. 1(a) and Fig. 2(a)). It was found that single-phase spinel powders can be obtained in the presence of CTAB

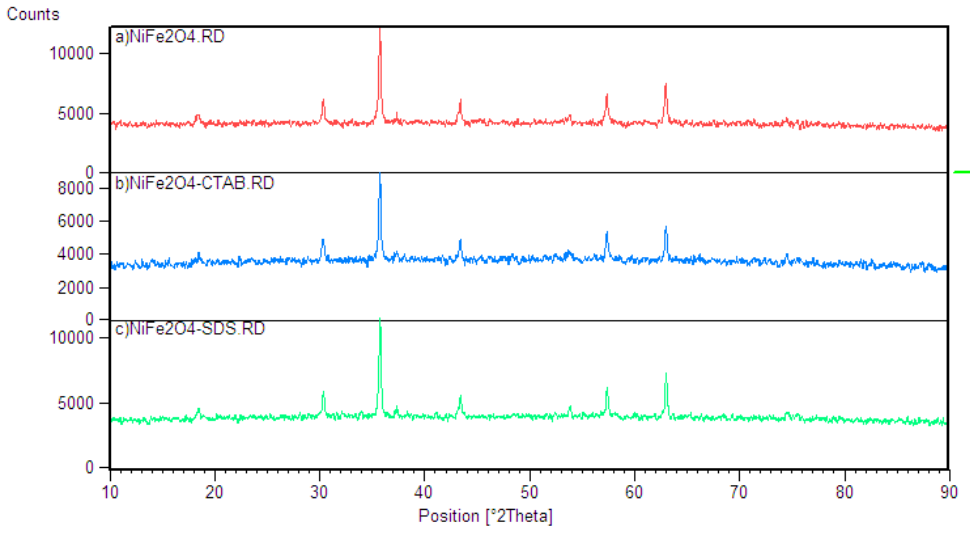

Fig. 2. XRD patterns of $NiFe_2O_4$ samples: a)$NiFe_2O_4$, b)$NiFe_2O_4$/CTAB & c)$NiFe_2O_4$/SDS.

(Fig. 1(b) and Fig. 2(b)) and SDS (Fig. 1(c) and Fig. 2(c)). The diffraction peaks at 2θ = 18.228 (1 1 1), 29.688 (2 0 2), 30.688 (2 2 0), 34.298 (3 1 0) 35.876 (3 1 1), 37.146 (2 2 2), 43.875 (4 0 0), 61.816 (4 0 4), and 86.689 (5 5 2) can be assigned to $CuFe_2O_4$ (ICDD card number 06–0545) and the diffraction peaks at 2θ = 21.583 (1 1 1), 35.699 (2 2 0), 43.353 (2 2 2), 50.709 (4 0 0), 63.682 (4 2 2), 67.399 (5 1 1), 74.485 (4 4 0) and 85.493 (6 2 0) can be assigned to $NiFe_2O_4$ (ICDD card number 44–1485). The mean crystallite size of the particles was determined by the XRD line width of (311) peak using Scherrer formula to be 50-95 nm (Table 1).

FT-IR analysis

FT-IR spectra of the samples are shown in Figs. 3 and 4.

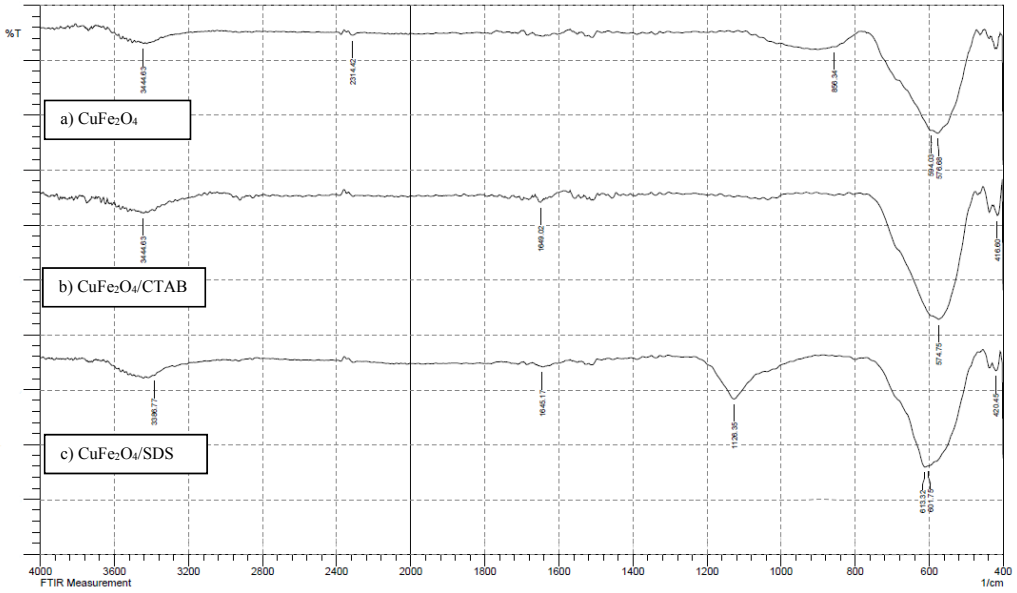

Fig. 3. FT-IR spectra of $CuFe_2O_4$ samples: a)$CuFe_2O_4$, b)$CuFe_2O_4$/CTAB & c)$CuFe_2O_4$/SDS.

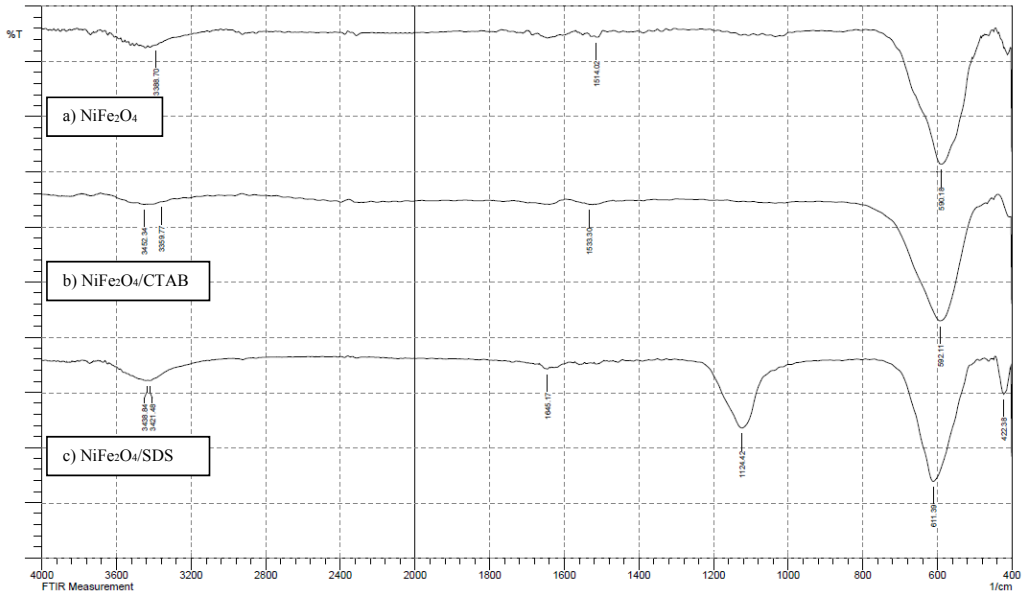

Fig. 4. FT-IR spectra of $NiFe_2O_4$ samples: a)$NiFe_2O_4$, b)$NiFe_2O_4$/CTAB & c)$NiFe_2O_4$/SDS.

The peaks at about 574-613 cm^{-1} and 416-422 cm^{-1} shown in Figs. 3 and 4 could be attributed to tetrahedral and octahedral complexes, respectively. The difference in the band positions is observed because of difference in the Fe^{3+}····O^{2-} distance for tetrahedral and octahedral complexes. It is clear that the intrinsic vibration of tetrahedral cluster is higher than that of octahedral cluster. The reason may be due to shorter bond lengths of the tetrahedral cluster compared to the octahedral cluster [28].

SEM analysis

The effect of surfactant on the morphology and size of the prepared samples has been studied. Figs. 5 and 6 show the SEM images of samples prepared without surfactant and using CTAB and SDS as surfactants. Completely agglomerated ferrite particles were obtained in the absence of any surfactant, shown in Fig. 5(a) and Fig. 6(a). It is clearly seen in the micrographs of Fig. 5(b) and Fig. 6(b) that in the presence of CTAB, the layered ferrite particles began to separate, and finally in the presence of SDS shown in Fig. 5(c) and Fig. 6(c), the particles possess individual pyramidal grains. In comparison with other samples, it was observed that the particles are single, roughly pyramidal and uniformly distributed crystals.

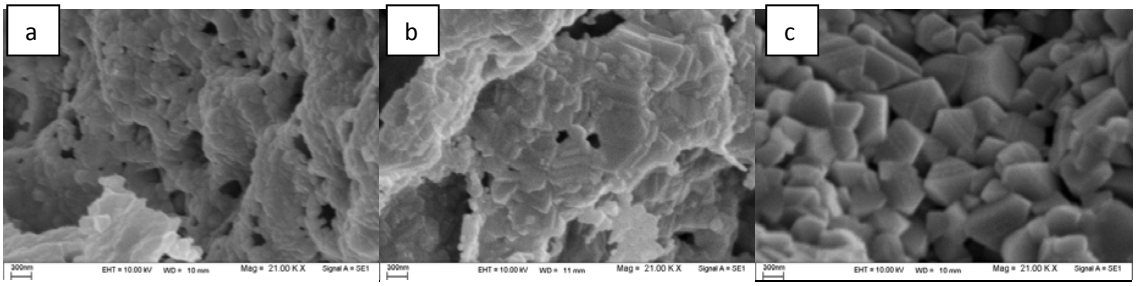

Fig. 5. SEM images of $CuFe_2O_4$ samples: a)$CuFe_2O_4$, b)$CuFe_2O_4$/CTAB & c)$CuFe_2O_4$/SDS.

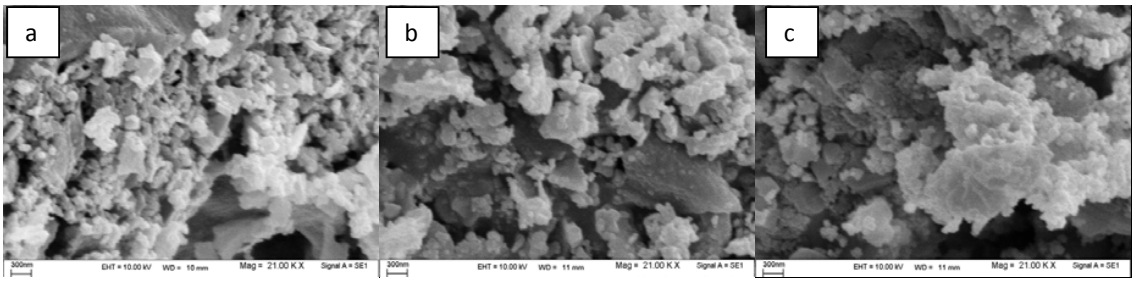

Fig. 6. SEM images of $NiFe_2O_4$ samples: a)$NiFe_2O_4$, b)$NiFe_2O_4$/CTAB & c)$NiFe_2O_4$/SDS.

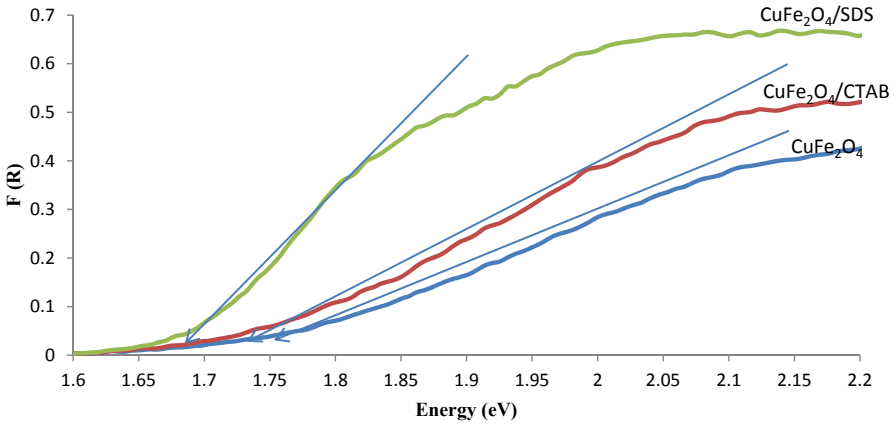

Fig. 7. The Kubelka–Munk plots of $NiFe_2O_4$ samples: a)$CuFe_2O_4$, b)$CuFe_2O_4$/CTAB & c)$CuFe_2O_4$/SDS.

Table 2. The calculated band gap energies of samples.

Copper ferrite samples	Band Gap/eV	Nickel ferrite samples	Band Gap/eV
$CuFe_2O_4$	1.75	$NiFe_2O_4$	1.71
$CuFe_2O_4$/CTAB	1.73	$NiFe_2O_4$/CTAB	1.76
$CuFe_2O_4$/SDS	1.68	$NiFe_2O_4$/SDS	1.77

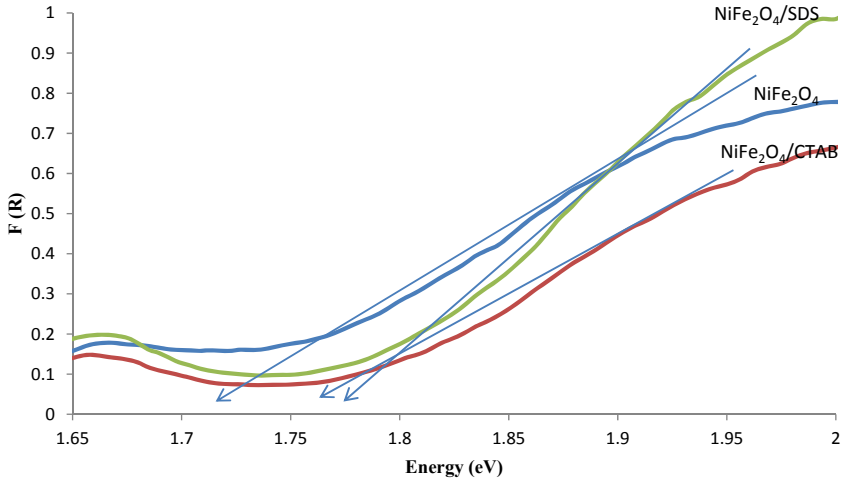

Fig. 8. The Kubelka–Munk plots of $CuFe_2O_4$ samples: a)$NiFe_2O_4$, b)$NiFe_2O_4$/CTAB & c)$NiFe_2O_4$/SDS.

DRS analysis

The analysis of optical absorption spectra is a powerful tool for understanding the band structure and band gap of both crystalline and noncrystalline materials. The optical properties of the ferrite samples were characterized by UV-DRS in addition with the optical absorption data.

The optical absorption coefficient (α) can be determined from the optical reflectance data with the Kubelka–Munk function (Eq. (1)):

$$\alpha = (1-R)^2/2R \quad (1)$$

where R is the diffuse reflectance. The optical band gap energy (E_g) for the synthesized samples was calculated with Tauc's relation (Eq. (2)):

$$\alpha h\nu = A\,(h\nu - E_g)^n \quad (2)$$

where hν is the excitation energy, A is a constant, n is an index that can be characterized in the optical absorption process, and α is the absorption coefficient. Figs. 7 and 8 show plots of $(\alpha h\nu)^2$ versus excitation energy (hν) in electron volts for all the synthesized samples. Extrapolation of the linear part of the Tauc plots to the intersection with the hν axis gives the values of E_g [29]. Therefore, the calculated band gap energies of samples were calculated and shown in Table 2, indicating that the samples may have visible-light photoactivity.

CONCLUSION

MFe_2O_4 (M= Cu and Ni) have been successfully synthesized by surfactant-assisted microwave sol-gel auto-combustion method with addition of cationic surfactant (CTAB and SDS). The combustion method is one of the facile and one-step methods. Using of microwaves in auto combustion method is economical and has notable features such as rapid heating rates and short processing durations. It was found that single-phase spinel powders can be obtained in the absence and presence of CTAB and SDS. Applying surfactants along with sol–gel method can improve the properties of the synthesized powders. In the presence of CTAB, the layered ferrite particles begin to separate, and in the presence of SDS, the particles possess individual pyramidal grains. The prepared samples shows an obvious absorption capability in the UV–Vis region, and the band-gap energy is between 1.68- 1.77 eV. They could be used as visible light responsive catalysts.

ACKNOWLEDGEMENTS

The authors acknowledge Iran University of Science & Technology, Institute for Color Science and Technology, South Tehran Branch of Islamic Azad University and Iranian Nanotechnology Initiative Council.

CONFLICT OF INTEREST

The authors declare that there is no conflict of interests regarding the publication of this manuscript.

REFERENCES

1. Sadri F, Ramazani A, Massoudi A, Khoobi M, Azizkhani V, Tarasi R, et al. Magnetic CoFe2O4 nanoparticles as an efficient catalyst for the oxidation of alcohols to carbonyl compounds in the presence of oxone as an oxidant. Bull Korean Chem Soc. 2014;35(7):2029.
2. Malekzadeh AM, Shokrollahi S, Ramazani A, Rezaei SJT, Asiabi PA, Joo SW. Synthesis of Hexabenzylhexaazaisowurtzitane (HBIW) under Ultrasound Irradiation with Fe3O4@ PCA Nanoparticles as an Efficient and Reusable Nanomagnetic Catalyst. Central European Journal of Energetic Materials. 2017;14(2):336-50.
3. Tarasi R, Khoobi M, Niknejad H, Ramazani A, Ma'mani L, Bahadorikhalili S, et al. β-cyclodextrin functionalized poly (5-amidoisophthalicacid) grafted Fe3O4 magnetic nanoparticles: A novel biocompatible nanocomposite for targeted docetaxel delivery. Journal of Magnetism and Magnetic Materials. 2016;417:451-9.
4. Ahankar H, Ramazani A, Joo SW. Magnetic nickel ferrite nanoparticles as an efficient catalyst for the preparation of polyhydroquinoline derivatives under microwave irradiation in solvent-free conditions. Research on Chemical Intermediates. 2016;42(3):2487-500.
5. Ramazani A, Sadri F, MASSOUDI A, Khoobi M, Joo SW, Dolatyari L, et al. Magnetic ZnFe2O4 nanoparticles as an efficient catalyst for the oxidation of alcohols to carbonyl compounds in the presence of oxone as an oxidant. Iranian Journal of Catalysis. 2015;5(3):285-91.
6. Fardood ST, Ramazani A, Moradi S. Green synthesis of Ni–Cu–Mg ferrite nanoparticles using tragacanth gum and their use as an efficient catalyst for the synthesis of polyhydroquinoline derivatives. Journal of Sol-Gel Science and Technology. 2017;82(2):432-9.
7. Taghavi Fardood S, Ramazani A, Golfar Z, Joo SW. Green synthesis of Ni-Cu-Zn ferrite nanoparticles using tragacanth gum and their use as an efficient catalyst for the synthesis of polyhydroquinoline derivatives. Applied Organometallic Chemistry. 2017:e3823-n/a.
8. Azizkhani V, Montazeri F, Molashahi E, Ramazani A. Magnetically Recyclable Cufe2o4 Nanoparticles as an Efficient and Reusable Catalyst for the Green Synthesis of 2,4,6,8,10,12-Hexabenzyl-2,4,6,8,10,12-hexaazaisowurtzitane as CL-20 Explosive Precursor. Journal of Energetic Materials. 2017;35(3):314-20.
9. Cullity BD, Graham CD. Introduction to magnetic materials: Hoboken, N.J. ; Chichester : Wiley ; IEEE Press; 2009.
10. Taghavi Fardood S, Ramazani A. Green Synthesis and Characterization of Copper Oxide Nanoparticles Using Coffee Powder Extract. Journal of Nanostructures. 2016;6(2):167-71.
11. Tianshu Z, Hing P, Jiancheng Z, Lingbing K. Ethanol-sensing characteristics of cadmium ferrite prepared by chemical coprecipitation. Materials Chemistry and Physics. 1999;61(3):192-8.
12. Li X, Zhu Z, Zhao Q, Wang L. Photocatalytic degradation of gaseous toluene over ZnAl2O4 prepared by different methods: A comparative study. Journal of Hazardous Materials. 2011;186(2):2089-96.
13. Cui Z-M, Chen Z, Jiang L-Y, Song W-G, Jiang L. A true nanocomposite: Single crystalline Au nanoparticles on single crystalline Fe3O4 nanoparticles. Materials Letters. 2011;65(1):82-4.
14. Amar IA, Lan R, Petit CTG, Arrighi V, Tao S. Electrochemical synthesis of ammonia based on a carbonate-oxide composite electrolyte. Solid State Ionics. 2011;182(1):133-8.
15. Xanthopoulou G, Vekinis G. Deep oxidation of methane using catalysts and carriers produced by self-propagating high-temperature synthesis. Applied Catalysis A: General. 2000;199(2):227-38.
16. Ghozza AM, El-Shobaky HG. Effect of Li2O-doping of CdO/Fe2O3 system on the formation of nanocrystalline CdFe2O4. Materials Science and Engineering: B. 2006;127(2):233-8.
17. Singh G, Kapoor IPS, Dubey R, Srivastava P. Preparation, characterization and catalytic behavior of CdFe2O4 and Cd nanocrystals on AP, HTPB and composite solid propellants, Part: 79. Thermochimica Acta. 2010;511(1):112-8.
18. Cordier A, Peigney A, De Grave E, Flahaut E, Laurent C. Synthesis of the metastable α-Al1.8Fe0.2O3 solid solution from precursors prepared by combustion. Journal of the European Ceramic Society. 2006;26(15):3099-111.
19. Fardood ST, Ramazani A, Moradi S. A NOVEL GREEN SYNTHESIS OF NICKEL OXIDE NANOPARTICLES USING ARABIC GUM. CHEMISTRY JOURNAL OF MOLDOVA. 2017;12(1):115-8.
20. Taghavi Fardood S, Ramazani A, Moradi S, Azimzadeh Asiabi P. Green synthesis of zinc oxide nanoparticles using arabic gum and photocatalytic degradation of direct blue 129 dye under visible light. Journal of Materials Science: Materials in Electronics. 2017;28(18):13596-601.
21. Fardood ST, Atrak K, Ramazani A. Green synthesis using tragacanth gum and characterization of Ni–Cu–Zn ferrite nanoparticles as a magnetically separable photocatalyst for organic dyes degradation from aqueous solution under visible light. Journal of Materials Science: Materials in Electronics. 2017;28(14):10739-46.
22. Samoila P, Cojocaru C, Sacarescu L, Dorneanu PP, Domocos A-A, Rotaru A. Remarkable catalytic properties of rare-earth doped nickel ferrites synthesized by sol-gel auto-combustion with maleic acid as fuel for CWPO of dyes. Applied Catalysis B: Environmental. 2017;202(Supplement C):21-32.
23. Sundararajan M, Kennedy LJ, Vijaya JJ, Aruldoss U. Microwave combustion synthesis of Co1−xZnxFe2O4 ($0 \le x \le 0.5$): Structural, magnetic, optical and vibrational spectroscopic studies. Spectrochimica Acta Part A: Molecular and Biomolecular Spectroscopy. 2015;140(Supplement C):421-30.
24. Sugimoto H, Daimatsu K, Nakanishi E, Ogasawara Y, Yasumura T, Inomata K. Preparation and properties of poly(methylmethacrylate)–silica hybrid materials incorporating reactive silica nanoparticles. Polymer. 2006;47(11):3754-9.
25. Ghobeiti Hasab M, Seyyed Ebrahimi SA, Badiei A. An investigation on physical properties of strontium hexaferrite nanopowder synthesized by a sol–gel auto-combustion process with addition of cationic surfactant. Journal of the European Ceramic Society. 2007;27(13):3637-40.
26. Dar MA, Batoo KM, Verma V, Siddiqui WA, Kotnala RK. Synthesis and characterization of nano-sized pure and Al-doped lithium ferrite having high value of dielectric constant. Journal of Alloys and Compounds. 2010;493(1):553-60.
27. Barati MR, Seyyed Ebrahimi SA, Badiei A. The role of surfactant in synthesis of magnetic nanocrystalline powder of NiFe2O4 by sol–gel auto-combustion method. Journal of Non-Crystalline Solids. 2008;354(47):5184-5.
28. Pradeep A, Chandrasekaran G. FTIR study of Ni, Cu and Zn substituted nano-particles of MgFe2O4. Materials Letters. 2006;60(3):371-4.
29. Shen Y, Wu Y, Li X, Zhao Q, Hou Y. One-pot synthesis of MgFe2O4 nanospheres by solvothermal method. Materials Letters. 2013;96(Supplement C):85-8.